Chin. J. Astron. Astrophys. Vol. 2 (2002), No. 1, 8–16
(http://www.chjaa.org or http://chjaa.bao.ac.cn)

Chinese Journal of
Astronomy and
Astrophysics

Properties of BL Lac Objects with Redshift $\leq$ 0.2

Ben-Zhong Dai[1,2,3] ⋆, Guang-Zhong Xie[1,2,3] and Ze-Jun Jiang [1,3]

[1] Yunnan Observatory, Chinese Academy of Science, Kunming 650011
[2] National Astronomical Observatories, Chinese Academy of Science, Beijing 100012
[3] Yunnan Astrophysics Center, Yunnan University, Kunming 650091

Received 2001 August 16; accepted 2001 December 10

Abstract We present a large sample which includes 82 BL Lac objects with redshifts below 0.2 from recent literature. We find strong correlations in both flux and luminosity between the radio (5 GHz) and optical bands (5500 Å). The correlations in other bands are very weak. Five TeV BL Lacs and two suspect sources are found to have similar properties as high-frequency-peaked BL Lacs (HBLs). Our results suggest that both the radio and optical emissions are from the same radiation mechanism in the SSC model. The TeV BL Lac candidates should be HBLs or HBL-like objects with small redshifts.

Key words: galaxies: active — BL Lacertae objects: general — gamma-ray: observations — radiation mechanisms: non-thermal

1 INTRODUCTION

Blazars, including BL Lacertae objects and Optical Violently Variable (OVV) quasars, belong to a class of active galactic nuclei (AGNs), the spectrum of which is dominated by nonthermal radiation from relativistic electrons in jets pointing at us (e.g. Blandford, & Rees 1978; Urry & Padovani 1995). The entire electromagnetic spectral energy distributions (SEDs) usually reveal two broad components, the low energy part, peaking in the IR to soft X-ray range, and the high energy part, peaking in the MeV – GeV – TeV range. Both components are variable, particularly the high energy component (Ulrich et al. 1997; Wehrle et al. 1998). Because BL Lacs were efficiently discovered in radio and X-ray surveys, they have been divided into two classes: X-ray selected BL Lacs (XBLs) and radio selected BL Lacs (RBLs). Recently, this terminology has been replaced by a classification scheme based on the broadband SED, and we now have "high-energy-peaked" BL Lacs (HBLs) and "low-energy-peaked" BL Lacs (LBLs). The division between the two classes is based on the ratio of the X-ray (1 keV) to radio (5 GHz) flux densities $f_{\rm x}/f_{\rm r}$ (e.g. Padovani & Giommi 1995), with a somewhat arbitrary dividing line at log $(f_{\rm x}/f_{\rm r}) \sim -5.5$ (Wurtz et al. 1995; Perlman et al. 1998). Most of XBLs are HBLs and most of RBLs are LBLs, although there are exceptions in both cases.

⋆ E-mail: bzdai@public.km.yn.cn

In recent years, high-energy γ-rays have come to play an important role in the studies of AGNs. Before the launch of the CGRO in 1991, the only known extragalactic source of high-energy γ-rays was 3C 273, which had been detected with the COS-B satellite 20 years ago (Swanenburg et al. 1978). The EGRET detector on board the CGRO has identified 66 AGNs that emit γ-rays at energies above 100 MeV (Hartman et al. 1999), and a substantial fraction of those sources still remain unidentified in the EGRET catalog and is likely to be also AGNs. In addition, five BL Lacs in total have been discovered to be TeV (>300 GeV) γ-rays sources (TBLs), all five are nearby objects with redshifts below 0.2, they are: Mrk 421 (z=0.031, Punch et al. 1992), Mrk 501 (z=0.034, Quinn et al. 1996), 1ES 2344+514 (z=0.044, Catanese et al. 1998), PKS 2155−304 (z=0.117, Chadwick et al. 1999), and 1ES 1959+650 (z = 0.048, Nishiyama. 1999). During flaring episodes, the γ-ray emission can greatly exceed the energy output of the AGN at all other wavelengths, and is always accompanied by flares in other bands. Until about ten years ago, the most viable radiation model for relativistic jets was the synchrotron-self-Compton (SSC) model (Marscher & Gear 1985; Ghisellini & Maraschi 1989). According to this model, the smooth, polarized and variable low-energy component of the blazar spectrum is produced by the synchrotron mechanism, while the high-energy component is caused by Comptonization of synchrotron radiation by the same population of electrons that produce the synchrotron component. There are some other models, however, such as the external-radiation-Compton (ERC) and hadronic models (Mannheim & Biermann 1992; Ghisellini & Madau 1996). In the hadronic models, the γ-rays are produced via synchrotron mechanism by secondary electrons which are much more energetic than the directly-accelerated electrons. The hadronic scenarios, as an alternative for the SSC model, have been proposed also to explain the TeV radiation, detected by atmospheric Cherenkov detectors in a number of low luminosity BL Lacs (TBLs).

Correlation between the radio and other energy band, especially the γ-ray in blazars has been widely studied (e.g., Stecker et al. 1993; Dondi, Ghisellini 1995; Mücke et al. 1997; Mattox et al. 1997; Zhou et al. 1997; Fan et al. 1998; Cheng et al. 2000; Zhang 2001). Maccagni et al. (1989) studied 35 X-ray selected BL Lacs, and obtained a tight correlation between the radio flux and the V magnitude, this correlation also holds for the new BL Lac objects found serendipitously in EXOSAT fields. The correlation between the X-ray and the radio flux is looser. Padovani et al. (1993) investigated the correlation of radio and optical luminosities for 19 RBLs and 29 XBLs. They found a correlation coefficient of 0.94 for the RBLs and one of 0.53 for the XBLs. Both the XBLs and RBLs have a positive correlation between radio and optical.

To study the broadband properties of the TBLs, we collected a sample of 82 objects with redshifts smaller than 0.2, because all five reported TBLs all have redshifts below 0.2. Section 2 presents the data, Section 3, their broadband properties. Section 4 gives a discussion and conclusions. Throughout this paper, we assume q_0=0.5, $H_0 = 75\,\mathrm{km\,s^{-1}Mpc^{-1}}$ and define spectral indices, α, such that $f_\nu \propto \nu^{-\alpha}$.

2 BROADBAND DATA OF BL LACS WITH REDSHIFTS BELOW 0.2

Our sample of BL Lac objects were selected from the literature (Perlman et al. 1996; Lin et al. 1996; Perlman et al. 1998; Landt et al. 2001; Nass et al. 1996; Laurent-Muehleisen et al. 1999; Rector et al. 2000). It contains a total of 82 objects with redshifts below 0.2. The redshift values and the radio fluxes have been updated by according to Veron-Cetty and

Veron (2000). The X-ray fluxes were converted to monochromatic flux at 1 keV assuming $\alpha_x = 1.0$ (Giommi et al. 1995). Using $B - V = 0.4$, (Padovani 1992) the B magnitudes were converted to V magnitudes for all objects. Table 1 lists, successively, (1) object name; (2) other name; (3) redshift; (4) V magnitude; (5) radio flux at 5 GHz (mJy); (6) X-ray flux at 1 keV (μJy); (7), (8) and (9) the two-point optical-to-X-ray and radio-to-optical spectral indices, $\alpha_{\mathrm{ro}} = \log(F_{5\,\mathrm{GHz}}/F_{5500\,\mathrm{\AA}})/5.04$, $\alpha_{\mathrm{ox}} = \log(F_{5500\,\mathrm{\AA}}/F_{1\,\mathrm{keV}})/2.65$ and the α_{rx}; and (10) the Compton luminosities at the high-energy peak (1 TeV). The relation between two broadband spectral indices can be written as $\alpha_{\mathrm{rx}} = 0.6554\,\alpha_{\mathrm{ro}} + 0.3446\,\alpha_{\mathrm{ox}}$. Our sample also includes the BL Lac objects detected by EGRET (Mukherjee 1997) with redshifts below 0.2 and the five TeV BL Lacs mentioned in the Introduction.

Table 1 The Sample of BL Lacs with Redshift below 0.2

Name	Alternative Name	z	m_V	F_{R} (mJy)	F_{x} (μJy)	α_{ox}	α_{ro}	α_{rx}	L_{c}
1ES0145+138[1]		0.125	17.9	5.67	4.406	0.665	0.268	0.404	0.322E+45
1ES0229+200[1]		0.139	14.68	49.09	2.260	1.260	0.198	0.564	0.204E+45
1ES0323+022[1]		0.147	17.4	42.0	3.520	0.777	0.400	0.530	0.356E+45
1ES0347−121[1]		0.188	18.2	9.0	4.638	0.611	0.331	0.428	0.767E+45
1ES0548−322[1],⋆	PKS	0.069	15.5	170.	5.864	0.980	0.370	0.580	0.130E+45
1ES0806+524[1]		0.138	15.0	171.9	2.760	1.179	0.331	0.623	0.247E+45
1ES0927+500[1]		0.188	17.2	18.34	1.348	0.964	0.313	0.538	0.223E+45
1ES1011+496[1]	1H	0.200	16.1	286.0	1.084	1.166	0.463	0.705	0.203E+45
1ES1101−232[1]	HEAO	0.186	16.1	66.0	7.258	0.854	0.336	0.515	0.117E+46
1ES1101+384[1],⋆	MRK421	0.031	14.4	722	7.834	1.098	0.407	0.646	0.351E+44
1ES1118+424[1]		0.124	17.0	35.0	2.818	0.874	0.353	0.532	0.203E+45
1ES1133+704[1]	MRK180	0.046	14.4	274.0	3.578	1.227	0.324	0.635	0.353E+44
1ES1212+078[1]		0.136	16.05	94.0	0.538	1.288	0.363	0.682	0.465E+44
1ES1218+285[1]	ON231	0.102	16.5	981.0	0.536	1.221	0.601	0.814	0.261E+44
1ES1218+304[1]		0.182	16.4	56.0	5.016	0.870	0.346	0.526	0.777E+45
1ES1239+069[1]		0.150	19.41	10.23	0.578	0.769	0.438	0.552	0.607E+44
1ES1255+244[1]		0.141	15.4	7.39	7.322	0.959	0.092	0.391	0.680E+45
1ES1312−423[1]		0.105	16.6	18.5	1.468	1.041	0.266	0.533	0.757E+44
1ES1426+428[1]	H	0.129	16.4	38.0	5.36	0.859	0.312	0.501	0.416E+45
1ES1440+122[1]		0.162	17.0	41.26	1.154	1.020	0.367	0.592	0.142E+45
1ES1652+398[1],⋆	MRK501	0.034	14.4	1371	7.404	1.108	0.463	0.685	0.399E+44
1ES1727+502[1]	I Zw187	0.055	16.7	159.0	2.144	0.964	0.460	0.633	0.303E+44
1ES1741+196[1]		0.083	16.6	222.6	2.260	0.970	0.481	0.649	0.728E+44
1ES1807+698[1]	3C371	0.051	14.2	2189.0	0.290	1.669	0.487	0.894	0.353E+43
1ES1959+650[1],⋆		0.048	13.67	251.6	7.296	1.220	0.259	0.590	0.787E+44
1ES2005−489[1],⋆	PKS	0.071	15.3	1192.0	4.256	1.063	0.522	0.708	0.100E+45
1ES2155−304[1],⋆	PKS	0.117	13.5	310.0	11.492	1.172	0.263	0.576	0.736E+45
1ES2200+420[1]	BL Lac	0.070	15.1	3593.0	1.498	1.264	0.601	0.830	0.344E+44
1ES2321+419[1]		0.059	17.0	19.0	0.542	1.144	0.300	0.591	0.883E+43
1ES2344+514[1],⋆		0.044	15.5	215.18	2.284	1.134	0.390	0.647	0.207E+44
1722+119[2]	4U	0.159	15.77	95.0	3.45	1.026	0.341	0.577	0.409E+45
1514+241[2]	AP LIB	0.048	14.80	1940.0	0.39	1.530	0.524	0.871	0.421E+43
0521−365[2]	PKS	0.055	14.62	8890.0	1.38	1.350	0.641	0.885	0.195E+44
0829+046[2]	OJ049	0.180	16.4	700.0	0.27	1.349	0.564	0.834	0.409E+44
2254+074[2]	OY091	0.190	16.36	480.0	0.51	1.250	0.528	0.777	0.862E+44
0245.2+1047[3]	WGA J	0.07	15.7	217.0	0.26	1.460	0.407	0.770	0.595E+43
0313.9+4115[3]	WGA J	0.029	17.0	48.0	0.11	1.405	0.380	0.733	0.433E+42
0428.8−3805[3]	WGA J	0.150	18.9	51.0	0.004	1.661	0.536	0.924	0.421E+42

Table 1 Continued

Name	Alternative Name	z	m_V	$F_{\rm R}$ (mJy)	$F_{\rm x}$ (μJy)	$\alpha_{\rm ox}$	$\alpha_{\rm ro}$	$\alpha_{\rm rx}$	$L_{\rm c}$
0513.8+0156[3]	WGA J	0.084	14.8	131.0	0.12	1.723	0.292	0.785	0.397E+43
0558.1+5328[3]	WGA J	0.036	14.0	234.0	0.04	2.024	0.279	0.880	0.242E+42
0816.0−0736[3]	WGA J	0.04	16.1	61.0	0.04	1.707	0.329	0.804	0.300E+42
1215+303[3]	ON325	0.130	15.6	478.0	0.27	1.469	0.467	0.812	0.213E+44
1811.7+3143[3]	EXO	0.117	17.4	127.0	0.09	1.378	0.496	0.800	0.576E+43
0847.2+1133[4]	WGA J	0.199	17.8	32.0	3.954	0.697	0.409	0.508	0.733E+45
1204.2−0710[4]	WGA J	0.185	17.6	128.0	0.07	1.389	0.512	0.814	0.112E+44
08054+7534[5]		0.121	18.1	26.0	3.06	0.694	0.415	0.511	0.210E+45
09168+5238[5]		0.190	19.5	36.0	2.21	0.536	0.554	0.548	0.373E+45
09306+4950[5]		0.186	18.0	15.0	10.72	0.504	0.359	0.409	0.174E+46
12302+2517[5]		0.135	15.6	289.0	1.379	1.202	0.424	0.692	0.118E+45
13410+3959[5]		0.163	18.5	33.0	2.753	0.651	0.467	0.530	0.341E+45
1418+546[5]	OQ530	0.152	15.65	1090.0	0.30	1.444	0.542	0.853	0.324E+44
RGB J0110+418[6]	RX J01100+4149	0.096	18.4	18.0	1.047	0.825	0.407	0.551	0.450E+44
RGB J0152+017[6]	PMN J 0152-0146	0.080	17.1	65.0	2.302	0.892	0.414	0.579	0.690E+44
RGB J0153+712[6]	8C 0149+710	0.080	17.7	291.0	1.263	0.899	0.591	0.697	0.378E+44
RGB J0214+517[6]	RX J02142+5144	0.049	17.9	161.0	5.26	0.635	0.556	0.583	0.590E+44
RGB J0314+247[6]	RX J03140+2445	0.054	18.3	6.0	0.596	0.932	0.304	0.521	0.813E+43
RGB J0654+427[6]	B3 0651+428	0.126	18.1	134.0	0.397	1.029	0.556	0.719	0.295E+44
RGB J0656+426[6]	4C+42.22	0.059	16.5	138.0	1.602	1.042	0.432	0.642	0.261E+44
RGB J0710+591[6]	1H0658+595	0.125	18.0	34.0	10.433	0.508	0.430	0.457	0.762E+45
RGB J1136+676[6]	RX J11365+6737	0.136	18.0	40.0	10.267	0.511	0.444	0.467	0.888E+45
RGB J1221+282[6]	W Comae	0.102	15.8	940.0	0.932	1.236	0.541	0.781	0.453E+44
RGB J1341+399[6]	RX J13410+3959	0.163	18.2	34.0	3.279	0.668	0.446	0.522	0.407E+45
RGB J1419+543[6]	S4 1418+54	0.151	15.0	1400.0	0.505	1.457	0.512	0.838	0.537E+44
RGB J1427+541[6]	RXJ14274+5409	0.105	17.4	24.0	0.331	1.164	0.352	0.632	0.171E+44
RGB J1428+436[6]	1H1430+423	0.130	16.9	21.0	25.42	0.528	0.301	0.379	0.201E+46
RGB J1516+293[6]	RX J15166+2917	0.130	18.2	34.0	0.803	0.898	0.446	0.602	0.634E+44
RGB J1532+302[6]	RXJ15319+3061	0.064	15.6	47.0	2.43	1.109	0.267	0.557	0.465E+44
RGB J1534+372[6]	RX J16347+3716	0.143	18.3	20.0	0.082	1.257	0.408	0.701	0.784E+43
RGB J1624+374[6]	B3 1746+470	0.200	19.4	14.0	0.104	1.052	0.465	0.667	0.195E+44
RGB J1725+118[6]	1H 1720+117	0.018	16.3	16.3	14.99	0.705	0.232	0.395	0.227E+44
RGB J1750+470[6]	B3 1748+470	0.160	19.0	10.0	1.66	0.658	0.404	0.492	0.199E+45
RGB J2250+384[6]	B3 2247+381	0.119	16.0	60.0	3.047	1.012	0.320	0.558	0.202E+45
RGB J2322+346[6]	RX J23226+3436	0.098	18.2	30.0	1.365	0.811	0.435	0.565	0.612E+44
MS0317.0+1834[7]		0.190	18.12	10.0	0.069	1.313	0.334	0.671	0.116E+44
MS0350.0−3712[7]		0.165	17.0	16.8	0.026	1.642	0.290	0.756	0.332E+43
MS1019.0+5139[7]		0.141	18.09	2.4	0.038	1.415	0.209	0.624	0.353E+43
MS1050.7+4946[7]		0.140	16.86	53.8	0.009	1.837	0.379	0.881	0.825E+42
MS1154.1+4255[7]		0.172	17.67	9.8	0.003	1.894	0.296	0.847	0.414E+42
MS1229.2+6430[7]		0.164	16.89	42.0	0.071	1.493	0.360	0.751	0.893E+43
MS1312.1−4221[8]		0.105	16.6	18.5	0.297	1.303	0.266	0.623	0.153E+44
MS2306.1+2236[7]		0.137	16.0	4.4	0.029	1.775	0.095	0.674	0.254E+43
MS2316.3−4222[7]		0.045	14.5	540.0	0.045	1.929	0.390	0.921	0.426E+42

Notes: [1] Perlman et al. 1996; [2] Lin et al. 1996; [3] Nass et al. 1996; [4] Landt et al. 2001; [5] Perlman et al. 1998; [6] Laurent-Muehleisen et al. 1999; [7] Rector et al. 2000.

Using $B-V=0.4$ and assuming $\alpha_{\rm o}=1.0$ (consistent with Stocke et al. 1991) to convert other optical band magnitudes to V-band magnitude. $\star$, this source is the TeV BL Lac objects or candidates. Chadwick et al. (2000) found 3σ limits to the VHE γ-ray flux of $0.39\times10^{-11}\,{\rm cm^{-2}\,s^{-1}}$ above 400 GeV for PKS 2005–489 and $2.4\times10^{-11}\,{\rm cm^{-2}\,s^{-1}}$ above 300 GeV for PKS 0548–322.

3 THE BROADBAND SPECTRAL PROPERTIES

From the available radio, optical and X-ray flux, we obtain the two-point indices $\alpha_{\rm rx}$, $\alpha_{\rm ro}$ and the $\alpha_{\rm ox}$ shown in Table 1. We follow Wurtz et al. (1995) and Perlman et al. (1998, 1999) in dividing the HBLs and LBLs according to the ratio of the X-ray (1 keV) to radio (5 GHz) flux densities $f_{\rm x}/f_{\rm r}$, somewhat arbitrarily at dividing line at $(\log f_{\rm x}/f_{\rm r}) \sim -5.5$. We also follow Perlman (1998) and Laurent-Muehleisen (1998, 1999) and refer objects in the range $-6.5 \leq \log(f_{\rm x}/f_{\rm r}) \leq -5.5$ ($0.72 \leq \alpha_{\rm rx} \leq 0.85$) as "intermediate" BL Lac objects (IBLs). The relation between $\log(f_{\rm o}/f_{\rm r})$ and $\log(f_{\rm x}/f_{\rm r})$ for our sample, is shown in Figure 1. There are three regions, for LBLs, ($\log(f_{\rm x}/f_{\rm r}) < -6.5$), IBLs, ($-6.5 \leq \log(f_{\rm x}/f_{\rm r}) \leq -5.5$), and HBLs ($\log(f_{\rm x}/f_{\rm r}) > -5.5$). Note that the values of $\log(f_{\rm x}/f_{\rm r})$ of the five TBLs and two suspect TBLs are > -5.5. From Table 2 we can see that the average values of the broadband indices, $\alpha_{\rm ox}$, $\alpha_{\rm ro}$, $\alpha_{\rm rx}$, are apparently different for the HBLs, LBLs, and IBLs. However, the values for the TBLs are close to those for the HBLs. This means that the TBLs detected up to now belong to HBLs. In addition, this also implies that future BL Lacs detected in TeV energy band would have similar properties to HBLs. This result is in agreement with the properties of TeV blazars observed by ground based instruments.

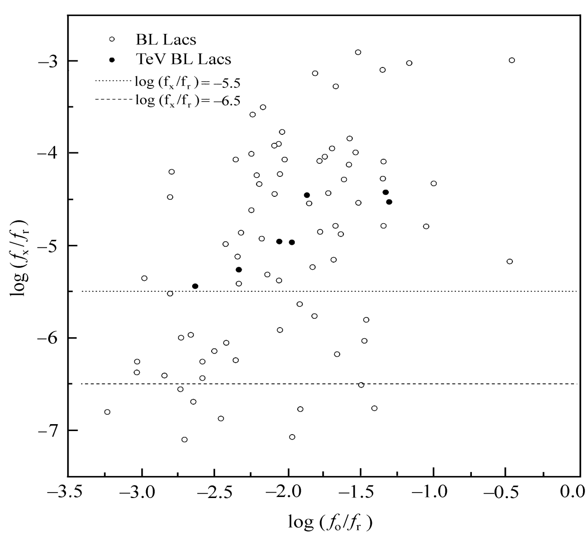

Fig. 1 Broadband properties of BL Lac objects. The open circles represent objects not detected in TeV energy band. The filled circle represent the confirmed TeV sources and candidates. The dotted line is $\log(f_{\rm x}/f_{\rm r}) = -5.5$, and the dashed line is $\log(f_{\rm x}/f_{\rm r}) = -6.5$.

In addition, we study the relations of broadband luminosities and radio, optical, and X-ray fluxes. As pointed out by Padovani (1992), because our sample is flux-limited, the luminosities are strongly correlated with redshifts, and would result in a spurious correlation. Therefore, we use a partial correlation analysis i.e., we examine the correlations between the radio and optical luminosities freed of the dependence on redshift. The correlation coefficients used for the analysis are the Spearman Rank-Order correlation coefficients (Press et al. 1992). A strong correlation between the radio and optical luminosities is found (see Figures 2, 3). The correlation coefficient between $\log L_{\rm o}$ and $\log L_{\rm r}$ for 82 BL Lacs is $\gamma = 0.64$, with $p < 10^{-4}$. The correlation coefficient between $\log f_{\rm o}$ and $\log f_{\rm r}$ for 82 BL Lacs is $\gamma = 0.66$, with $p < 10^{-4}$. The flux and luminosity correlations between these two bands are

$$\log L_{\rm r} = (0.838 \pm 0.113) \times \log L_{\rm o} + (6.733 \pm 3.305)\,, \tag{1}$$

and

$$\log f_{\rm r} = (0.842 \pm 0.106) \times \log f_{\rm o} + (1.985 \pm 0.062)\,. \tag{2}$$

No correlation was found between $L_{\rm x}$ and $L_{\rm r}$ or $L_{\rm o}$. Maccagni et al. (1989) also obtained a tight correlation between radio flux and optical magnitudes. This suggests that the radiations of radio and optical energy band are from the same radiation mechanism.

Table 2 The Average Values of Broadband Properties of LBLs, IBLs, HBLs, and TeV BL Lacs (TBLs)

Average	HBLs	IBLs	LBLs	TBLs
$\alpha_{\rm ox}$	0.96	1.40	1.70	1.15
$\alpha_{\rm ro}$	0.37	0.47	0.53	0.36
$\alpha_{\rm rx}$	0.57	0.79	0.88	0.63
numbers	56	17	9	7

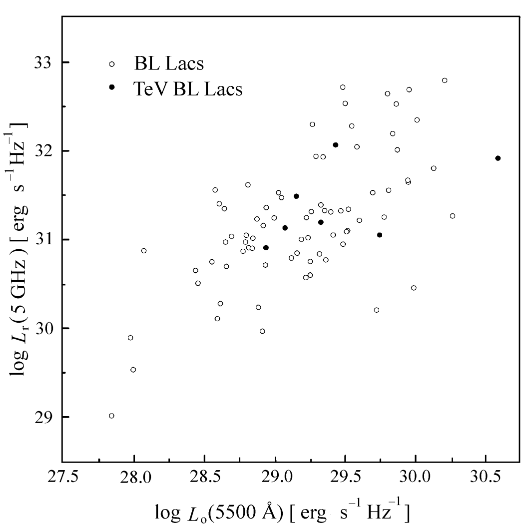

Fig. 2 Correlation between optical (5500 Å) and radio (5 GHz) luminosities. The meaning of symbols is the same as Figure 1.

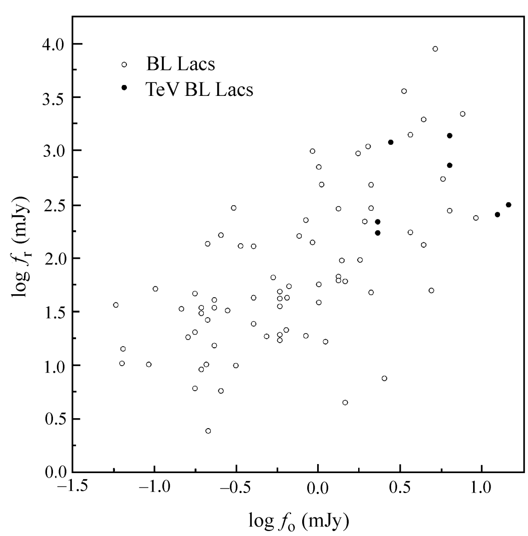

Fig. 3 Correlation between optical (5500 Å) and radio (5 GHz) fluxes. Meaning of symbols same as in Figure 1.

4 THE TWO PEAK FREQUENCIES AND LUMINOSITIES

The γ-ray-loud BL Lac objects (FSRQs similar to LBLs) have some common properties which imply physical similarities. It is believed that the γ-ray emission from TBLs is dominated by the synchrotron self-Compton (SSC) process. Within the present uncertainties, the low-frequency side of each of the two peaks of TBLs can be described by the same spectral index (Tavecchio et al. 1998), consistent with the SSC model. In the context of SSC model, the peak frequencies of the synchrotron component $\nu_{\rm s}$ and the Compton component $\nu_{\rm c}$ are related: $\nu_{\rm c}/\nu_{\rm s} \propto \gamma_{\rm peak}^2$, where $\gamma_{\rm peak}$ is the characteristic electron energy. For TBLs, the averaged upshifting factor of the Compton peak relative to the synchrotron peak is $\sim 10^{8\pm1}$, i.e.,

$$\frac{\nu_{\rm c}}{\nu_{\rm s}} \simeq 10^{8\pm1} \,. \tag{3}$$

The luminosities ($L_{\rm s}$, $L_{\rm c}$), peak luminosities ($L_{\rm s}(\nu_{\rm s})$ and $L_{\rm c}(\nu_{\rm c})$), and peak flux densities ($f_{\rm s}(\nu_{\rm s})$ and $f_{\rm c}(\nu_{\rm c})$) of the two components are related by (Tavecchio et al. 1998; Stecker et al. 1996)

$$\frac{L_{\rm c}}{L_{\rm s}} = \frac{\nu_{\rm c} L_{\rm c}(\nu_{\rm c})}{\nu_{\rm s} L_{\rm s}(\nu_{\rm s})} = \frac{\nu_{\rm c} f_{\rm c}(\nu_{\rm c})}{\nu_{\rm s} f_{\rm s}(\nu_{\rm s})} \,. \tag{4}$$

During the high state, the five TBLs all have a Compton luminosity $L_{\rm c}$ comparable to or slightly less than the synchrotron luminosity $L_{\rm s}$, i.e., $L_{\rm c}/L_{\rm s} \sim 1$. In the low state, the value of this ratio is almost 0.1 (Urry et al. 1999). Assuming this is valid for the candidate TeV sources, we obtain

$$\nu_{\rm c} L_{\rm c}(\nu_{\rm c}) \simeq \nu_{\rm s} L_{\rm s}(\nu_{\rm s}) \,. \tag{5}$$

Since the flux sensitivity of TeV γ-ray detectors is not high, it is necessary for a candidate TeV source to have a peak in its Compton component in the TeV γ-ray energy range in order to be detected. BL Lac (2200+420, z=0.069) itself is one of the brightest LBLs. It has a Compton radiation peak in the GeV energy range (Fossati et al. 1998) and is a strong GeV γ-ray source, but it was not detected in the TeV energy range even during a large optical/GeV outburst in July/August 1997 (Bloom et al. 1997; Bai et al. 1999; Aharonian et al. 2000). Therefore, TeV candidates should be selected from among HBLs or HBL-like objects. We assume the synchrotron emission peak at 1 keV (2.42×10^{17} Hz), and the Compton emission peak at 1 TeV. According to equations (3) to (5), all the HBLs in our sample give $\nu_{\rm c}/\nu_{\rm s} = 10^9$, and their Compton emission peak luminosities, $L_{\rm c}$, consistent with the observations, are shown in Table 1.

5 DISCUSSION AND CONCLUSIONS

Dondi & Ghisellini (1995) investigated the correlations between emissions in γ-ray and in the lower energy bands, and found that the γ-ray luminosity is more tightly correlated with the radio luminosity than with other bands luminosities (e.g. optical and X-ray); but Mücke et al. (1997) reported that there is no correlation between the γ-ray and the radio. As pointed out by Lu et al. (1997) and Padovani (1992), the optical and correlated with the core radio luminosity than with the total radio luminosity. Xie et al. (1997) found that the luminosity correlation between the γ-ray and the infrared is closer than that between the γ-ray and the optical or the X-ray. Fan (1998) thought that the luminosity-luminosity correlation could not be considered as a true correlation because of the well known fact that the luminosity depends on the redshift. In this paper, we consider both the flux-flux and the luminosity-luminosity correlation between the radio, optical, and X-ray energy for our sample with redshifts below 0.2. We find strong correlation between the optical and the radio both in flux and luminosity. The correlations among other bands are very weak.

Two alternative explanations have been proposed for the difference between HBLs and LBLs. The "orientation hypothesis" argues that these sources have no significant physical differences, and that the differences in luminosity and spectra result from the relativistic beaming effects, with the jets of HBLs being observed at larger angles to the line of sight (Maraschi et al. 1986; Urry, Padovani & Stickel 1991; Celotti et al. 1993). In the alternative interpretation, the difference between HBLs and LBLs must be attributed, at least in part, to real physical differences (Giommi & Padovani 1994; Padovani & Giommi 1995; Sambruna et al. 1996): the X-ray emission comes from the high-energy end of the synchrotron emission for the HBLs, and from Compton scattering for the LBLs. If real difference exists between the HBLs and LBLs, then one might expect that HBLs rather than LBLs are likely to be TeV sources. This is because there is evidence that in the synchrotron SED relativistic electrons are accelerated to higher energies in HBLs than in LBLs (Sambruna et al. 1996). These electrons, in turn, should be Compton-scattered to produce higher energy γ-rays in HBLs than in LBLs. Our result of luminosities in high energy peak is in agreement with all of the existing TeV BL Lacs observations, and so support the real difference hypothesis. We further predict that only nearby HBLs (say, $z \leq 0.2$) can be extragalactic TeV sources.

Acknowledgements Our sincere thanks to the referee for valuable comments and suggestions that helped us to improve our presentation. This work was financially supported by the National Natural Science Foundation of China and Natural Science Foundation of Yunnan Province (2000A004M).

References

Aharonian F. A., Akhperjanian A. G., Barrio J. A. et al., 2000, A&A, 353, 847
Bai J. M., Xie G. Z., Li K. H. et al., 1999, A&AS, 136, 455
Blandford R. D., Rees M. J., 1978, In: A. N. Wolfe, ed., Pittsburgh Conference on BL Lac Objects, Pittsburgh: University of Pittsburgh Press, 328
Bloom S. D., Bertsch D. L., Hartman R. C. et al., 1997, ApJ, 490, L145
Catanese M., Akerlof C. W., Badran H. M. et al., 1998, ApJ, 501, 616
Celotti A., Maraschi L., Ghisellini G. et al., 1993, ApJ, 416, 118
Chadwick P. M., Daniel M. K., Lyons K. et al., 2000, A&A, 364, 450
Chadwick P. M., Lyons K., McComb T. J. L. et al., 1999, ApJ, 513, 161
Cheng K. S., Zhang X., Zhang L., 2000, ApJ, 537, 80
Dondi L., Ghisellini G., 1995, MNRAS, 273, 583
Fan J. H., Adam G., Xie G. Z. et al., 1998, A&A, 338, 27
Fossati G., Maraschi L., Celotti A. et al., 1998, MNRAS, 299, 433
Ghisellini G., Madau P., 1996, MNRAS, 280, 67
Ghisellini G., Maraschi L., 1989, ApJ, 340, 181
Giommi P., Padovani P., 1994, MNRAS, 268, L51
Giommi P., Ansari S. G., Micol A., 1995, A&AS, 109, 267
Hartman R. C., Bertsch D. L., Bloom S. D. et al., 1999, ApJS, 123, 79
Landt H., Padovani P., Perlman E. S. et al., 2001, MNRAS, 323, 757

Laurent-Muehleisen S. A., Kollgaard R. I., Feigelson E. D. et al., 1999, ApJ, 525, 127
Laurent-Muehleisen S. A., Kollgaard R. I., Ciarullo R. et al., 1998, ApJS, 118, 127
Lin Y. C., Bertsch D. L., Dingus B. L. et al., 1996, A&AS, 120, 499
Lu Y., Wang T., 1997, In: Bradley M. Peterson, Fu-zhen Cheng, Andrew S. Wilson., eds., ASP Conf. Ser. 113: IAU Colloq. 159, Emission Lines in Active Galaxies: New Methods and Techniques, p.252
Maccagni D. et al., 1989, In: L. Maraschi, T. Maccacaro, M. H. Ulrich, eds., BL Lac Objects, 334, p.287
Mannheim K., Biermann P. L., 1992, A&A, 253, L21
Maraschi L., Ghisellini G., Tanzi E. G. et al., 1986, ApJ, 310, 325
Marscher A. P., Gear W. K., 1985, ApJ, 298, 114
Mattox J. R. et al., 1997, ApJ, 481, 95
Mücke A., Pohl M., Reich P. et al., 1997, A&A, 320, 33
Mukherjee R., Bertsch D. L., Bloom S. D. et al., 1997, ApJ, 490, 116
Nass P., Bade N., Kollgaard R. I. et al., 1996, A&A, 309, 419
Nishiyama T., Ghamoto N., Chikawa M. et al., 1999, Proc. 26th ICRC, 1, 370
Padovani P., 1992, A&A, 256, 399
Padovani P. et al., 1993, MNRAS, 260, L21
Padovani P., Giommi P., 1995, ApJ, 444, 567
Perlman E. S., Padovani P., Giommi P. et al., 1998, AJ, 115, 1253
Perlman S. M., Stocke J. T., Schachter J. F. et al., 1996, ApJS, 104, 251
Press W., Flannery B., Teukolsky S. et al., 1992, Numerical Recipes: The Art of Scientific Computing 2nd ed., Cambridge: Cambridge Univ. Press
Punch M., Akerlof C. W., Cawley M. F. et al., 1992, Nature, 358, 477
Quinn J., Akerlof C. W., Biller S. et al., 1996, ApJ, 456, L83
Rector T. A., Stocke J. T., Perlman E. S. et al., 2000, AJ, 120, 1626
Sambruna R. M., Maraschi L., Urry C. M., 1996, ApJ, 463, 444
Stecker F. W., Salamon M. H., Malkan M. A., 1993, ApJ, 410, L71
Stecker F., De Jager O. C., Salamon M. H., 1996, ApJ, 473, L75
Swanenburg B. N., Bennett K., Bignami G. F. et al., 1978, Nature, 275, 298
Tavecchio F., Maraschi L., Ghisellini G., 1998, ApJ, 509, 608
Ulrich M.-H., Maraschi L., Urry C. M., 1997, AR&AA, 35, 445
Urry C. M., Padovani P., 1995, PASP, 107, 803
Urry C. M., Padovani P., Stickel M., 1991, ApJ, 382, 501
Urry C. M., Astroparticle Physics, 11, 159, (astro-ph/9903189)
Veron-Cetty M.-P., Veron P., A Catalogue of Quasars and Active Nuclei, 2000, ESO Scientific Report
Wehrel A. E., Pian E., Urry C. M. et al., 1998, ApJ, 497, 178
Wurtz R. E., Stocke J. T., Yee H. K. C., 1996, ApJS, 103, 109
Xie G. Z., Zhang Y. H., Fan J. H., 1997, ApJ, 477, 114
Zhang L., Cheng K. S., Fan J. H., 2001, PASJ, 47, 265
Zhou Y. Y., Lu Y. J., Wang T. G. et al., 1997, ApJ, 484, L47